# Optimized Soil-Footing Interaction Analysis for Edge Footings Subjected to Eccentric Loading

**Anurag Saraogi[1*], Vivek Garg[1], S.K. Dubey[1]**

[1]Civil Engineering Department Maulana Azad National Institute of Technology, Bhopal, India
Corresponding Author. Email: anurag.saraogi16@gmail.com

**Abstract**
Footings subjected to eccentric loading often experience significant challenges such as uneven pressure distribution, excessive tilt, and differential settlement—particularly for columns located at the edge or corner of a structure. This study proposes a novel, performance-based optimization approach using modified geometries of footings to address these issues effectively and economically. Three innovative configurations are introduced: Isolated Footing with Insertion (IFI), Tapered Footing with Insertion (TFI), and Trapezoidal Tapered Footing with Insertion (TTFI). These designs aim to enhance stability, reduce tilt, and ensure uniform pressure distribution while maintaining or reducing the overall volume of concrete required. Using finite element modeling on ANSYS for Soil-Footing interaction (SFI) analysis, the performance of each configuration is evaluated and compared against conventional isolated footings. The results reveal that the TTFI configuration offers superior performance, achieving near-uniform pressure distribution and significantly reduced tilt without increasing volume and geometrical modifications involving insertions and tapering can provide a safe, efficient, and economical solution to the longstanding problem of footing instability under eccentric loads

**Keyword:** Eccentric Load, Finite Element Method, Pressure Distribution, Settlement, Tilt.

## 1. Introduction

Shallow foundations remain a fundamental component in civil engineering due to their cost-effectiveness and ease of construction. However, under eccentric and inclined loading conditions, which often arise from seismic forces, lateral earth pressure, structural misalignment, or proximity to property boundaries, their behavior becomes increasingly complex and unpredictable [1,2]. Such loads result in non-uniform stress distributions beneath the footing, leading to partial contact loss, foundation tilt, and a marked reduction in bearing capacity [3,4]. Traditional bearing capacity theories, including those developed by Terzaghi and Meyerhof, assume vertical and centric loads and thus provide limited accuracy when applied to eccentric or inclined load scenarios [5,6].

To address these limitations, various studies have examined the performance of footings subjected to non-centric loads. Advanced modeling has demonstrated that the limit load space of rigid strip footings on cohesive-frictional soils reduces significantly as eccentricity increases [7]. Similarly, numerical studies on strip footings embedded in nonhomogeneous clays show that eccentric loading alters failure mechanisms and reduces ultimate bearing capacity [4].

To counteract the adverse effects of such loading, researchers have proposed geometric modifications to the footing base. T-shaped footings, characterized by a central vertical insert extending into the soil, have emerged as an effective solution for resisting both sliding and overturning [1]. These inserts increase passive resistance, improve confinement, and enhance load-settlement performance. Studies employing experimental testing and soft computing models have found that T-shaped footings can offer up to four times the bearing capacity of conventional strip footings under similar eccentricities [3]. Other designs, such as E-shaped, angle-shaped, and skirted footings, have also shown promise by altering pressure distributions and improving performance under inclined and eccentric loading [8,9,18].

The depth of vertical projection plays a crucial role in foundation stability. Deeper inserts enhance confinement, delay the onset of shear failure, and reduce tilt [15,16]. Angle-shaped footings that extend toward the eccentric load side offer better rotational resistance, particularly when embedded in reinforced or dense sand [2,17]. These configurations redistribute stress more efficiently and can be optimized for specific eccentricity ratios (e/B), embedment depths (D/B), and soil types [19]. In addition to geometric interventions, improvements to the supporting soil have been explored. Reinforced soil beds using geogrids and confinement techniques have shown enhanced bearing capacity and reduced settlement under eccentric-inclined loads [10,11]. Foundations with expanded bases or ring shapes supported on reinforced soil layers provide better stability, especially over soft or unsaturated soils [12,13]. Experimental studies confirm that even dense sand can exhibit early failure under eccentric vertical loads, emphasizing the importance of effective design solutions [14].

Finite element tools, such as OptumG2, have enabled precise upper and lower bound limit analyses to understand complex interactions between footing geometry and soil behavior under combined loading [21]. These numerical techniques have been instrumental in analyzing footing responses under varying levels of eccentricity and inclination, providing insights into failure envelopes and stress trajectories [6,20]. Despite these advancements, the practical

application of modified footings is limited by the absence of standardized design methodologies, especially in codes that primarily consider vertical centric loads [15]. Moreover, the lack of empirical validation for many innovative shapes in real soil conditions further limits their adoption.

To overcome these limitations, this study introduces three novel geometries—Isolated Footing with Insertion (IFI), Tapered Footing with Insertion (TFI), and Trapezoidal Tapered Footing with Insertion (TTFI)—designed to address high eccentricity while minimizing tilt, improving pressure uniformity, and maintaining or reducing footing volume. These configurations are evaluated using validated FEM-based SFI modeling in ANSYS, with performance compared against traditional footings under the same boundary and loading conditions. In Fig. 1, the footings of boundary line columns F1 and F2 are subject to eccentric loading. Footing F1 experiences eccentricity in both directions, while footing F2 is subjected to eccentricity in only one direction. This study focuses on footing F2. Due to its one-directional eccentricity, the pressure beneath the column is higher at the edge near the column and gradually reduces toward the opposite edge. Consequently, the required thickness and width of the footing differ at both ends. The design is therefore based on the variation in thickness and width to safely resist the resulting pressure distribution.

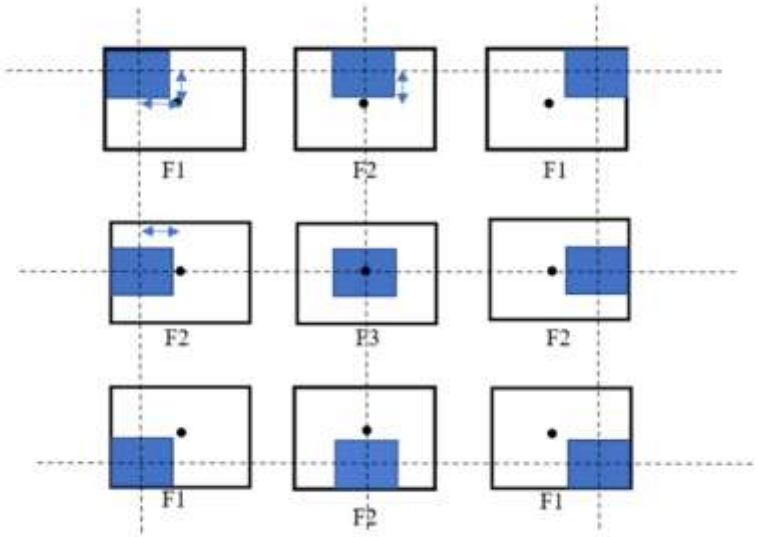


F1= Corner Footing, F2= Edge footing, F3= Centre footing

**Fig. 1 Centre line plan of Footing Arrangements**

## 2. Problem for Investigation

Footings located at the edge or corner of a boundary line are affected by tilting, uneven settlement, and irregular pressure distribution due to high eccentric loading. Aim of this study to reduce settlement and unevenness of pressure distribution with the help of Isolated Footing (IF), Isolated Footing with Insertion (IFI), Tapered Footing with Insertion (TFI), and Trapezoidal Tapered Footing with Insertion (TTFI).

### 2.1. Material Property

A Soil-Foundation interaction analysis is conducted for various types of concrete footings resting on soil, assuming linear soil behavior. Table 1 provided soil and footing material properties used in and additional size of soil domain also mentioned

**Table 1 Soil and Footing Properties and Dimension of Soil**

| **Parameters** | **Values** |
|---|---|
| Soil Elasticity (E) | 25 MPA |
| Poisson Ratio | 0.3 |
| Soil Domain Size | 20m x 20m x 10m |
| Footing Material | Concrete |
| Elasticity of Concrete | 25000 MPA |
| Poisson Ratio of Concrete | 0.17 |

### 2.2. Modeling of Footings

The finite element method (FEM) was used to analyze the Soil-Foundation interaction by dividing it into smaller elements to calculate displacements, stresses, and strains under applied loading conditions. SOLID186 (20-node hexahedral) elements were used in regular regions, and SOLID187 (10-node tetrahedral) elements were applied near irregular boundaries like the soil-structure interface. The footing dimensions were taken as shown in Figure 2, with a mesh size of 200 mm for the footing and 500 mm for the surrounding soil to ensure accurate and efficient results.

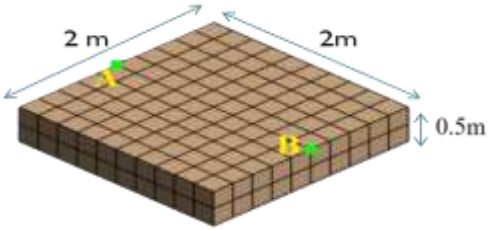


(a) Isolated Footing (IF)

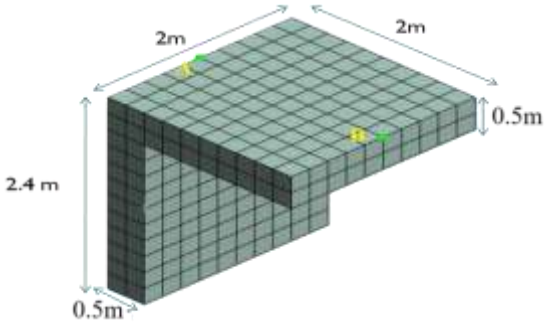


(b) Isolated Footing with Insertion (IFI)

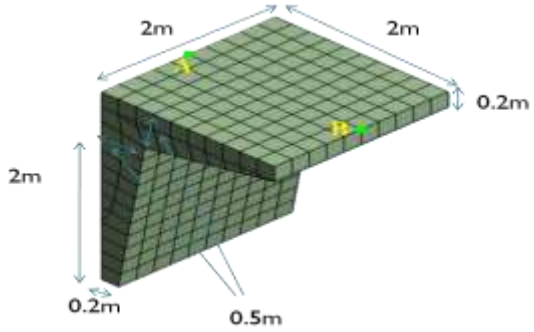


(c) Tapered Footing with Insertion (TFI)

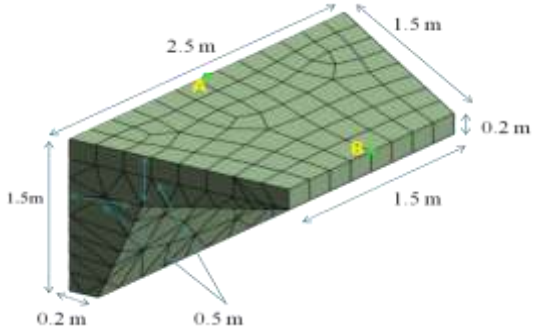


(d) Trapezoidal Tapered Footing with Insertion

**Fig.2 Dimension of footing and footing with insertion for SFI Analysis**

### 2.3. Loading on Footings

The axial load from the column is transferred to the footing through the center of the column. For a corner column with a width of 400 mm, this means the load is applied 200 mm from the left edge of the footing, as shown in Fig. 3.

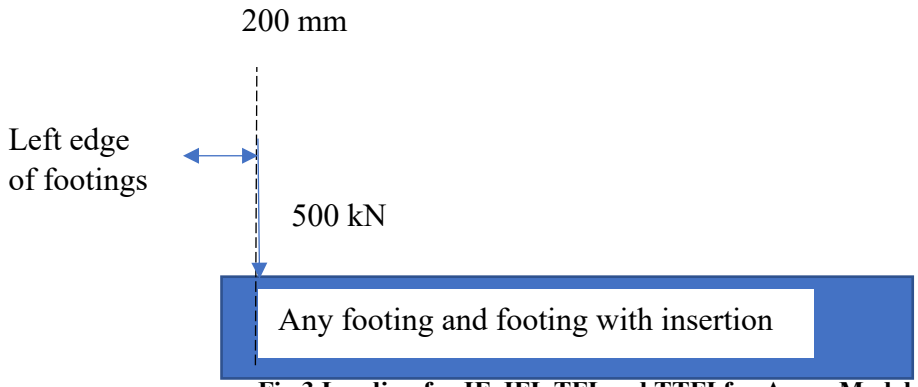


**Fig.3 Loading for IF, IFI, TFI and TTFI for Ansys Model**

## 3. Validation of Software

Immediate settlement of isolated footing due to concentric vertical load provided in IS 8009:1976, as per this code immediate settlement given by

$$\text{Settlement (y)} = \frac{QB(1-\mu^2)I_F}{E_S} \quad (1)$$

Here Q = Pressure (Load/Area) on footing, B= width of footing, $I_F$ = Influence Factor, $\mu$ = Poisson's ratio, $E_S$ = Elasticity of Soil

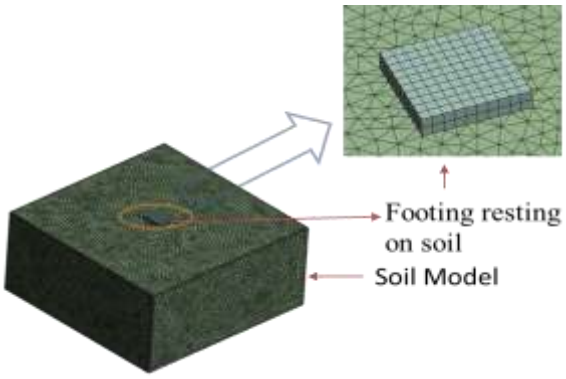


**Fig.4 Soil-Foundation Interaction model of Isolated footing**

Figure 4, used for validation, a soil domain measuring 10 m × 10 m × 10 m with an isolated footing subjected to a 100 kN load. Two footing configurations are analyzed: one measuring 1 m × 1 m × 0.01 m to examine flexural behavior, and another measuring 1 m × 1 m × 0.5 m to represent rigid behavior. The analysis is conducted using ANSYS Finite Element Analysis, with a mesh size of 500 mm for the soil and 200 mm for the concrete footing. Settlement values are calculated using Equation 1 and compared with the numerical results obtained from the simulation for both footing configurations. The comparison of ANSYS results is presented in Table 2.

**Table 2 Settlement at center and corner result validation**

| Footing | Size (m) | Deformation in Y-direction (mm) | | | | Percentage Variation in Ansys Result | |
|---|---|---|---|---|---|---|---|
| | | Ansys | | Theoretical | | | |
| | | Center | Corner | Center | Corner | Center | Corner |
| Flexible footing | 1*1*0.01 | 3.56 | 2.00 | 4.07 | 2.04 | 0.13 | 0.02 |
| Rigid footing | 1*1*0.5 | 2.80 | 2.80 | 2.98 | 2.98 | 0.06 | 0.06 |

## 4. Result and Discussion

Soil-Foundation interaction (SFI) Analysis of Isolated Footing (IF), Isolated Footing with Insertion (IFI), Tapered Footing with Insertion (TFI), and Trapezoidal Tapered Footing with Insertion (TTFI) under eccentric loading and result of relative settlement, tilt and volume on basic of these result performances of footing observed.

### 4.1. Relative Settlement and Tilt analysis for different case of footings

Relative settlement is defined as the difference in settlement between points A and B, which are indicated in Figure 2. Tilt is calculated as the relative settlement per unit width

**Table 3 Relative settlement, Tilt and Volume for IF, IFI, TFI and TTFI**

| Sr. No. | Geometry | Relative Settlement (mm) | | Relative Settlement in mm ($S_a$ - $S_b$) | Tilt (in $10^{-3}$) | Volume ($m^3$) |
|---|---|---|---|---|---|---|
| | | at A ($S_a$) | at B ($S_b$) | | | |
| 1 | Isolated Footing (IF) | -13.10 | -3.60 | -9.50 | -4.8 | 2 |
| 2 | Isolated Footing with insertion (IFI) | -5.18 | -3.36 | -1.82 | -0.9 | 4 |
| 3 | Tapered Isolated Footing with Insertion (TFI) | -4.87 | -3.26 | -1.61 | -0.8 | 2.95 |
| 4 | Trapezoidal Tapered Footing with Insertion (TTFI) | -5.89 | -4.45 | -1.44 | -1.0 | 2 |

Table 3 presents the Relative Settlement, Tilt, and Volume of IF, IFI, TFI, and TTFI footings under eccentric loading. The highest tilt value, $4.8 \times 10^{-3}$, is observed for IF. However, this can be reduced using IFI, TFI, and TTFI configurations. For IFI, the tilt is reduced to $0.9 \times 10^{-3}$, but the volume of the footing increases from 2 $m^3$ to 4 $m^3$. In the case of TFI, the tilt is further reduced to $0.8 \times 10^{-3}$ with only a slight increase in volume from 2 $m^3$ to 2.95 $m^3$. For TTFI, the tilt can be reduced to $1 \times 10^{-3}$ without any increase in the footing volume. These improvements happen because the modified shapes help move the center of gravity closer to the point of loading, which reduces the effect of eccentricity and lowers the tilt. Also, the inserted parts of the footing push against the surrounding soil and generate passive earth pressure, which helps resist the load and adds extra stability.

### 4.2. Pressure Distribution below the various Footings

Pressure below the footing for IF, IFI, TFI and TTFI were calculated with the help of ANSYS and validate the result of IF with the formula P/A ± M/Z.

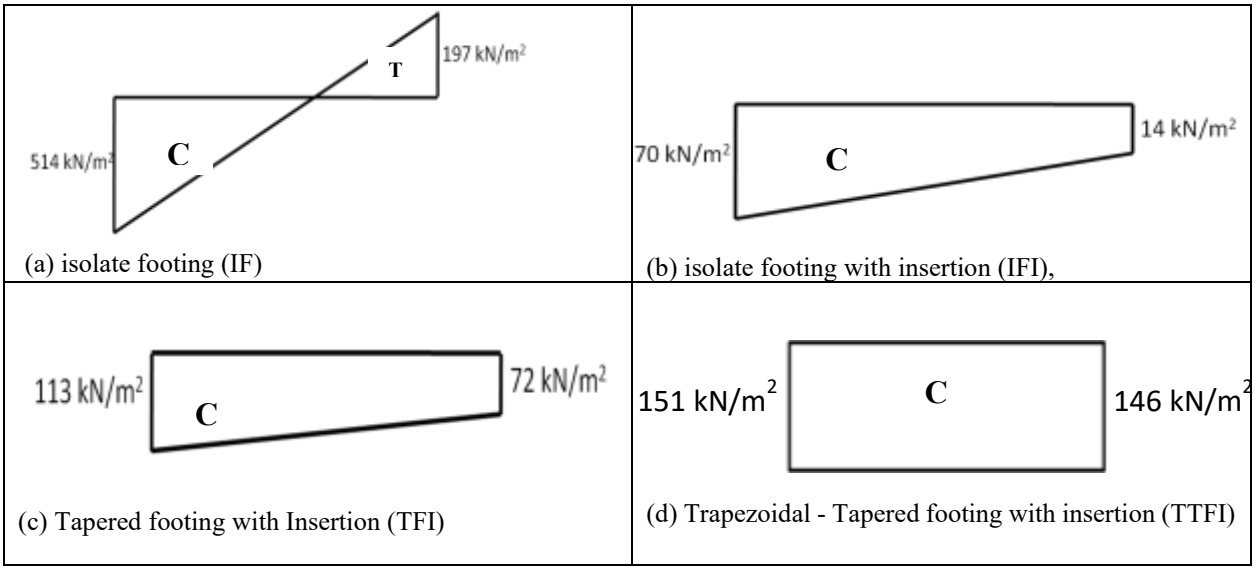


Here, C= Compression, T= Tension

**Fig.5 Pressure distribution below the IF, IFI, TFI and TTFI along the width of footing**

The figure 5 (a) shows how pressure is distributed along sections A and B of the Isolated Footing (IF)**.** The pressure is not uniform, meaning it is unevenly spread across the footing. On the right side, there is tension, which means the footing is pulling away from the soil. The maximum tension in this area is 197 kPa, which increases the risk of the footing tilting because it loses proper contact with the ground. On the left side, there is high compressive pressure, reaching 514 kPa, where the footing is pressing heavily on the soil. This imbalance in pressure—tension on one side and high compression on the other—can make the footing unstable and may cause it to tilt or settle unevenly.

The figure 5 (b) shows the pressure distribution below the isolated footing with insertion. The tension in the footing is reduced due to the insertion, making the footing more stable. However, the pressure is still slightly non-uniform, varying from 70 kPa to 14 kPa along section AB, as shown in the figure. The pressure below the footing is low, and the volume is larger than that of the isolated footing. This suggests an opportunity to reduce the volume and make the pressure more uniform.

The figure 5 (c) shows the pressure distribution below the tapered footing with insertion (TFI) along section AB. The volume of the TFI is reduced with the help of tapering in footing and insertion, and the pressure is more uniform compared to the isolated footing with insertion (IFI). In this footing, the pressure varies from 113 kPa to 72 kPa, which is still non-uniform but shows better uniformity than the IFI. The lower pressure magnitude and the reduced volume indicate an opportunity to further optimize the design and achieve more uniform pressure distribution.

The figure 5 (d) shows the pressure distribution of the trapezoidal-tapered footing with insertion (TTFI) along section AB. The volume of this footing is reduced due to the combined effect of the trapezoidal and tapered shapes. This design makes the pressure more uniform while maintaining the same volume as the isolated footing (IF). The pressure in the TTFI is lower and more uniform compared to the IF, varying only slightly from 151 kPa to 146 kPa.

## 5. Conclusion

After conducting an Soil-Foundation interaction (SFI) study on Isolated Footing (IF), Isolated Footing with Insertion (IFI), Tapered Footing with Insertion (TFI), and Trapezoidal Tapered Footing with Insertion (TTFI) under eccentric loading, the analysis reveals the following key conclusions:

1. The study demonstrates that modifying the geometry of footings through insertion and tapering significantly improves their stability and performance under eccentric loading. The addition of insertion reduces the effects of tension, making the footing more stable by preventing excessive tilting and uneven settlement.
2. The inclusion of insertion in isolated footings reduces tension forces and improves pressure uniformity. This modification enhances the footing's stability by minimizing the difference between compressive and tensile forces, thereby reducing the risk of tilting.
3. The use of tapered and trapezoidal shapes in combination with insertion further enhances the pressure distribution. These geometrical modifications help reduce the overall volume of the footing while making the pressure more uniform. The improved uniformity ensures better load transfer to the soil, reducing the chances of differential settlement and enhancing the overall structural efficiency.
4. The trapezoidal-tapered footing with insertion (TTFI) demonstrates the best performance among the analyzed configurations. It achieves a nearly uniform pressure distribution with reduced tilt and without any increase in footing volume. This makes TTFI the most stable and efficient design for handling eccentric loads.

**Compliance with ethical standards**

**Conflict of interest**
On behalf of all authors, the corresponding author states that there is no conflict of interest.

## References


1. Kaya N., & Ornek M. (2013). Experimental and numerical studies of T-shaped footings. Acta Geotechnica Slovenica, 10(1), 43–58.
2. Mahiyar H., & Patel A. N. (2000). Analysis of angle shaped footing under eccentric loading. Journal of Geotechnical and Geoenvironmental Engineering, 126(12), 1151–1156. https://doi.org/10.1061/(ASCE)1090-0241(2000)126:12(1151)
3. Kounlavong K., Sadik L., Keawsawasvong S., & Jamsawang P. (2024). Optimized CatBoost-based soft-computing models for prediction of the ultimate bearing capacity of T-shaped footings. Arabian Journal for Science and Engineering. https://doi.org/10.1007/s13369-024-09379-7
4. Zatar N., Baazouzi M., Bouaicha A., et al. (2024). Numerical investigation study on the performance of strip footing under eccentric loading condition embedded in nonhomogeneous clay soils. Indian Geotechnical Journal, 55(2), 690–700. https://doi.org/10.1007/s40098-024-01006-4
5. Meyerhof G. G. (1953). The bearing capacity of foundations under eccentric and inclined loads. In Proceedings of the 3rd ICSMFE (pp. 440–445).
6. Das B. M. (1980). Eccentrically loaded surface footing on sand layer resting on rough rigid base. Transportation Research Record, 827, 41.
7. Pham Q. N., Ohtsuka S., Isobe K., & Fukumoto Y. (2022). Limit load space of rigid strip footing on cohesive-frictional soil subjected to eccentrically inclined loads. Computers and Geotechnics, 151, 104956. https://doi.org/10.1016/j.compgeo.2022.104956
8. Sadoglu E., Cure E., Moroglu B., & Uzuner B. A. (2009). Ultimate loads for eccentrically loaded model shallow strip footings on geotextile-reinforced sand. Geotextiles and Geomembranes, 27(3), 176–182. https://doi.org/10.1016/j.geotexmem.2008.11.002
9. Pham Q. N., Ohtsuka S., Isobe K., Fukumoto Y., & Hoshina T. (2019). Ultimate bearing capacity of rigid footing under eccentric vertical load. Soils and Foundations, 59(6), 1980–1991. https://doi.org/10.1016/j.sandf.2019.09.004
10. Halder K., & Chakraborty D. (2020). Effect of inclined and eccentric loading on the bearing capacity of strip footing placed on the reinforced slope. Soils and Foundations, 60(4), 791–799. https://doi.org/10.1016/j.sandf.2020.04.006
11. Li C., Zhou A., & Jiang P. (2020). Eccentric bearing capacity of embedded strip footings placed on slopes. Computers and Geotechnics, 119, 103352. https://doi.org/10.1016/j.compgeo.2019.103352
12. Patra C. R., Das B. M., Bhoi M., & Shin E. C. (2006). Eccentrically loaded strip foundation on geogrid-reinforced sand. Geotextiles and Geomembranes, 24(4), 254–259. https://doi.org/10.1016/j.geotexmem.2005.12.001
13. Nawghare S. M., Pathak S. R., & Gawande S. H. (2010). Experimental investigations of bearing capacity for eccentrically loaded footing. International Journal of Engineering Science and Technology, 2(10), 5257–5264.
14. Musso A., & Ferlisi S. (2009). Collapse of a model strip footing on dense sand under vertical eccentric loads. Geotechnical and Geological Engineering, 27, 265–279. https://doi.org/10.1007/s10706-008-9227-y
15. Srinivasan V., & Ghosh P. (2012). Experimental investigation on interaction problem of two nearby circular footings on layered cohesionless soil. Geomechanics and Geoengineering, 1–10. https://doi.org/10.1080/17486025.2012.695401
16. Laman M., & Yildiz A. (2007). Numerical studies of ring foundations on geogrid-reinforced sand. Geosynthetics International, 14(2), 52–64. https://doi.org/10.1680/gein.2007.14.2.52

17. Joshi D. P., & Mahiyar H. K. (2009). Effectiveness of angle shaped footings resting on soil under eccentric inclined load. International Journal of Theoretical Applied Mechanics, 4(1), 95–105.
18. Saran S., Kumar S., Garg K., et al. (2007). Analysis of square and rectangular footings subjected to eccentric-inclined load resting on reinforced sand. Geotechnical and Geological Engineering, 25, 123–137. https://doi.org/10.1007/s10706-006-0010-7
19. Loukidis D., Chakraborty T., & Salgado R. (2008). Bearing capacity of strip footings on purely frictional soil under eccentric and inclined loads. Canadian Geotechnical Journal, 45(6), 768–787. https://doi.org/10.1139/T08-015
20. Georgiadis M. (1993). Settlement and rotation of footings embedded in sand. Soils and Foundations, 33(2), 169–175. https://doi.org/10.3208/sandf1972.33.169
21. Bransby M. F., & Randolph M. F. (1998). Combined loading of skirted foundations. Géotechnique, 48(5), 637–655. https://doi.org/10.1680/geot.1998.48.5.637